

UC Berkeley

UC Berkeley Previously Published Works

Title

Surface- and bulk-micromachined two-dimensional scanner driven by angular vertical comb actuators

Permalink

<https://escholarship.org/uc/item/8cm3g6n1>

Journal

Journal of Microelectromechanical Systems, 14(6)

ISSN

1057-7157

Authors

Piyawattanametha, W
Patterson, P R
Hah, D
[et al.](#)

Publication Date

2005-12-01

Peer reviewed

Surface- and Bulk- Micromachined Two-Dimensional Scanner Driven by Angular Vertical Comb Actuators

Wibool Piyawattanametha, *Member, IEEE*, Pamela R. Patterson, *Member, IEEE*, Dooyoung Hah, Hiroshi Toshiyoshi, *Member, IEEE*, and Ming C. Wu, *Fellow, IEEE*

Abstract—In this paper, we present the design, fabrication, and measurements of a two-dimensional (2-D) optical scanner with electrostatic angular vertical comb (AVC) actuators. The scanner is realized by combining a foundry-based surface-micromachining process (Multi-User MEMS Processes—MUMPs) with a three-mask deep-reactive ion-etching (DRIE) postfabrication process. The surface-micromachining provides versatile mechanical design and electrical interconnect while the bulk micromachining offers high-aspect ratio structures leading to flat mirrors and high-force, large-displacement actuators. The scanner achieves dc mechanical scanning ranges of $\pm 6.2^\circ$ (at 55 Vdc) and $\pm 4.1^\circ$ (at 50 Vdc) for the inner and outer gimbals, respectively. The resonant frequencies are 315 and 144 Hz for the inner and the outer axes, respectively. The 1-mm-diameter mirror has a radius of curvature of over 50 cm. [1454]

Index Terms—Angular vertical comb (AVC) actuators, confocal microscopy two-dimensional (2-D) scanner, electrostatic force actuators, laser beam steering, micromirror, optical coherence tomography (OCT), scanner.

I. INTRODUCTION

ADVANCES in optical microelectromechanical systems (MEMS) technology have made it possible to realize compact, batch-fabricated, and cost-effective optical scanning components. In recent years, electrostatically actuated one-dimensional (1-D) and two-dimensional (2-D) scanners have been widely used in applications such as optical telecommunication subsystems [1]–[4], barcode scanners [5], projection displays [6], and endoscopic microscopy [7]–[10], owing to their low power consumption, low cost, and ease of integration. The general requirements of scanners for these applications are

optically flat mirrors (radius of curvature more than 0.5 m), moderate actuation voltage (less than 100 V), and high reliability (more than a billion cycles). Endoscopic microscopy, including optical coherence tomography (OCT) and confocal microscopy, presents a unique challenge for MEMS scanners. Large mirror area and wide scan range are needed to achieve high-resolution imaging, at the same time a small footprint is necessary for the probe to fit in standard endoscope ports [7]–[11]. Three-dimensional endoscopic imaging in OCT imaging applications requires 2-D scanning. This is realizable by either cascaded 1-D scanners or a single 2-D scanner. The latter is preferable because it simplifies the optical system and reduces the overall packaging size [10].

Recently, there has been increasing interest in vertical comb-actuated 2-D scanners [1], [12]–[15]. The vertical comb actuators offer large force and extensive vertical displacement. The pull-in instability found in many electrostatic actuators can also be avoided when they are properly designed [16]. Two-dimensional scanners have been realized on a single device layer of a silicon-on-insulator (SOI) wafer [12], [13], [15]. Other approaches employing two SOI layers have also been reported [1], [14]. Electrical isolation and mechanical coupling among SOI structures are accomplished by using polysilicon-filled trenches [12], or backside islands [13]. Flip-chip bonding technique is employed for electrical interconnect [1]. Some scanners can only operate in resonant mode due to the small difference in comb finger thicknesses [12]. Other scanners operated in dc as well as resonant modes [1], [13]–[15].

Previously, we have reported 1-D scanners with angular vertical combdrive (AVC) actuators fabricated by bulk-micromachining [17] and hybrid surface- and bulk-micromachining processes [18]. Compared with conventional staggered vertical combdrive actuators [1], [13]–[15], the AVC offers inherent self-alignment between the movable and the fixed comb fingers because they are patterned by a single lithography and etching step. Furthermore, larger scan angles can be achieved for the same finger dimensions [16]. To extend the use of AVCs to 2-D scanners, multiple (at least three) electrical interconnect lines need to be routed through the mechanical springs of the gimbal frame to the inner AVCs. This is difficult in single-layer SOIs because all torsion springs are electrically shorted to the mirror.

Here, we report on the realization of 2-D AVC scanners using a hybrid surface-/bulk- micromachining process. The bulk-micromachined SOI structures offers large, flat mirrors and powerful actuators; while the surface-micromachined polysilicon structures provide versatile electrical wiring, hinges, locking mechanism, and compliant torsion springs. Furthermore, it has

Manuscript received November 3, 2004; revised April 20, 2005. This work was supported by NSF Biophotonics Program under Grant BES-0119. W. Piyawattanametha, P. R. Patterson, D. Hah, H. Toshiyoshi, and Ming C. Wu, "A 2D scanner by surface and bulk micromachined angular vertical comb actuators," in *OMEMS 2003, IEEE/LEOS Int. Conf. on Optical MEMS*, HI, USA, 2003, pp. 93–94. Subject Editor C. H. Mastrangelo.

W. Piyawattanametha was with the Department of Electrical Engineering, University of California, Los Angeles, CA 90095 USA. He is now with National Electronics and Computer Technology Center (NECTEC), 12120 Thailand, and Stanford University, CA 94305 USA (e-mail: wibool@stanford.edu).

P. R. Patterson was with the Department of Electrical Engineering, University of California, Los Angeles, CA 90095 USA. He is now with HRL Laboratories, CA 90265 USA.

D. Hah and M. C. Wu were with the Department of Electrical Engineering, University of California, Los Angeles, CA 90095 USA. They are now with Department of Electrical Engineering and Computer Sciences, University of California, Berkeley, CA 94720 USA (e-mail: dyhah@icsl.ucla.edu; wu@eecs.berkeley.edu).

H. Toshiyoshi is with the Institute of Industrial Science, University of Tokyo, Tokyo 153-8505, Japan (e-mail: hiro@iis.u-tokyo.ac.jp).

Digital Object Identifier 10.1109/JMEMS.2005.859073

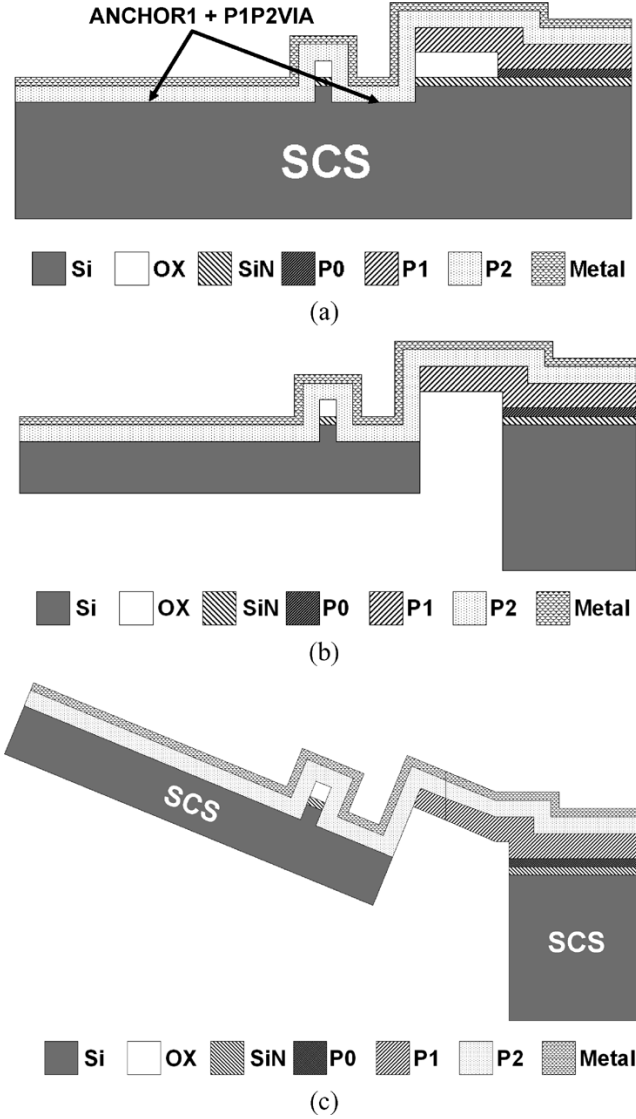


Fig. 2. Cross sections of a comb finger: (a) before postfabrication, (b) after postfabrication, and (c) after assembly.

on the geometry and dimensions of the cross section. For rectangular torsion springs, K has the form

$$K = \frac{w_s^3 t_s}{3} \left[1 - \frac{192 w_s}{\pi^5} \frac{t_s}{t_s} \tanh \left(\frac{\pi}{2} \cdot \frac{t_s}{w_s} \right) \right], \quad \text{for } w_s < t_s \quad (2)$$

where w_s (width), t_s (thickness), and l_s (length) are the torsion spring parameters. From (1) and (2), a thin and long beam allows us to achieve a compliant torsion spring.

B. Comb Drive Design

When an electrical bias is applied, an electrostatic torque, T_e is generated between fixed comb fingers and movable comb fingers. The overlapping area between comb fingers increases with electrical bias while the gap spacing between comb fingers remains unchanged. T_e can be written as

$$T_e(\theta, V) = N_{\text{finger}} V^2 \frac{\partial C_{\text{unit}}(\theta)}{\partial \theta} \quad (3)$$

where V is the electrical bias voltage between the movable and the fixed combs, C_{unit} is the capacitance per unit length between

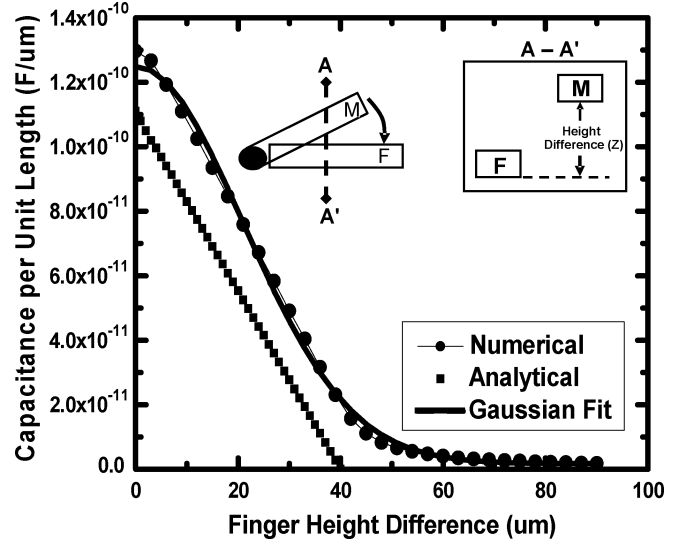


Fig. 3. The calculated unit capacitance per unit length versus the finger offset. The inset shows the cross section of the finger pair.

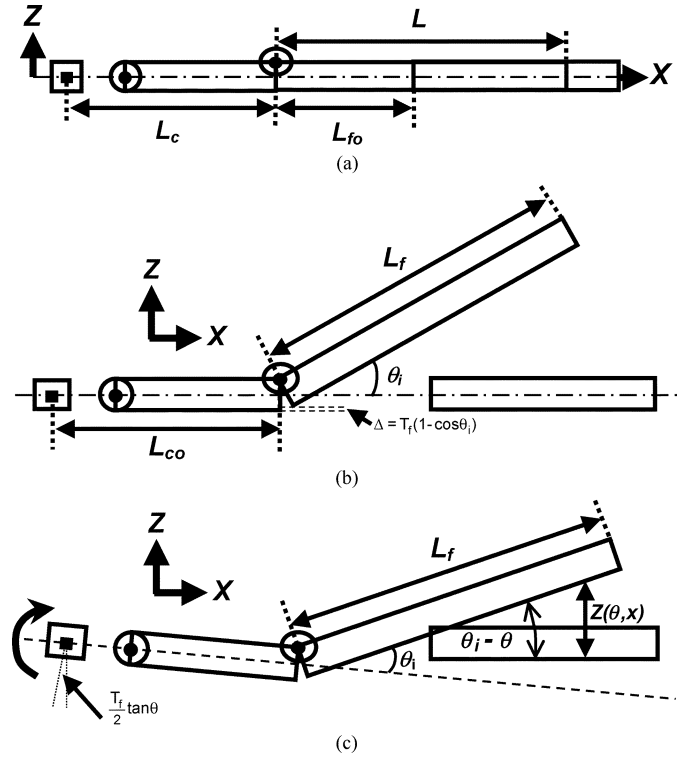


Fig. 4. Cross section of a movable comb finger (a) before assembly, (b) after assembly, and (c) under actuation.

a movable and a fixed finger, and N_{finger} is the number of movable fingers in each comb.

The C_{unit} is estimated using a 2-D finite element method (using FEMLAB from COMSOL, Inc.), which takes into account the fringe fields (not negligible in AVC actuators) between comb fingers [16]. The resulting C_{unit} as a function of the finger offset is shown in Fig. 3. The inset shows the cross section of the movable (denoted M) and the fixed comb (denoted F) fingers. The C_{unit} calculated using parallel plate actuator model without considering the fringe fields is also plotted in Fig. 3. It has lower capacitance value than that obtained from the numerical model. These numerically calculated C_{unit} are

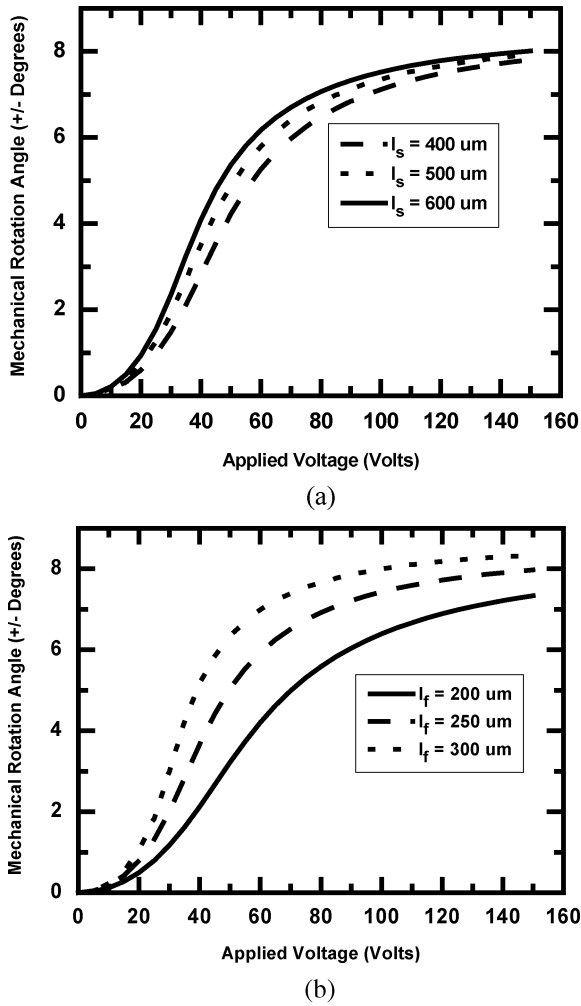


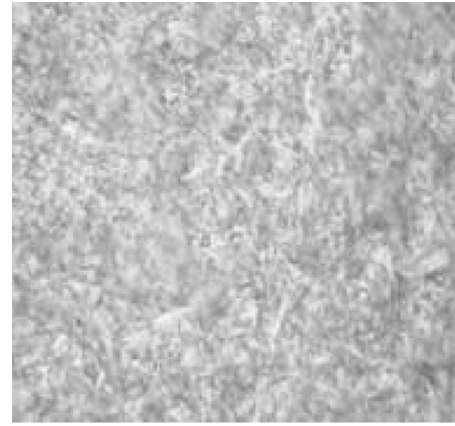
Fig. 5. Calculated dc scanning characteristics for (a) various spring lengths and (b) various comb finger lengths.

TABLE I
PARAMETERS OF THE SCANNER

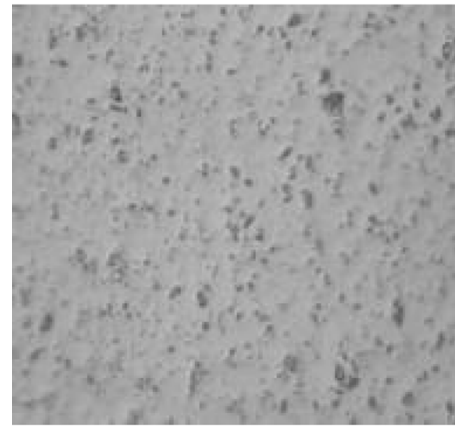
Parameters	Expression	Nominal Values
Mirror and comb finger thicknesses	T_m, T_f	35 μm
Inner torsion beam width	w_{si}	10 μm
Inner/Outer torsion beam length	l_{si}, l_{so}	345 μm
Outer torsion beam width	w_{so}	12 μm
Inner/Outer torsion beam thickness	t_s	3.5 μm
Initial angle	θ_i	10°
Comb finger size	w_f	4.6 μm
Comb finger length	L_f	242 μm
Comb finger gap spacing	g_f	4.4 μm
Movable comb finger clearance	L_{fo}	135 μm
Movable comb finger offset	L_{co}	35 μm
Number of movable and fixed comb fingers	N_{finger}	10, 11
Latch length	l_l	105 μm
Latch width	w_l	36 μm
Latch thickness	t_l	1.5 μm

fitted by a Gaussian function of the form shown in (4) by a least-mean-square-error fit:

$$C_{\text{unit}}(z) = C_1 + C_2 \exp(-C_3 z^2) \quad (4)$$



(a)



(b)



(c)

Fig. 6. Optical micrographs of the back surface after (a) lapping in 9- μm Al_2O_3 , and polishing in (b) 1- μm Al_2O_3 , and (c) colloidal silica.

where C_1 , C_2 , and C_3 are the fitting parameters dependent on the geometry of the comb finger. The total capacitance, C_t , can then be estimated analytically by integrating along the comb fingers overlapping area. The detailed calculation process can be found in [16].

As shown in Fig. 4, the movable combs are offset from the axis of rotation defined by the torsion spring. The integration of C_{unit} needs to take into account this offset. Fig. 4(a)–(c) shows the movable comb finger before assembly, after assembly, and with an electrical bias, respectively. Z is the vertical (along z -axis) distance between the movable and the fixed comb, mea-

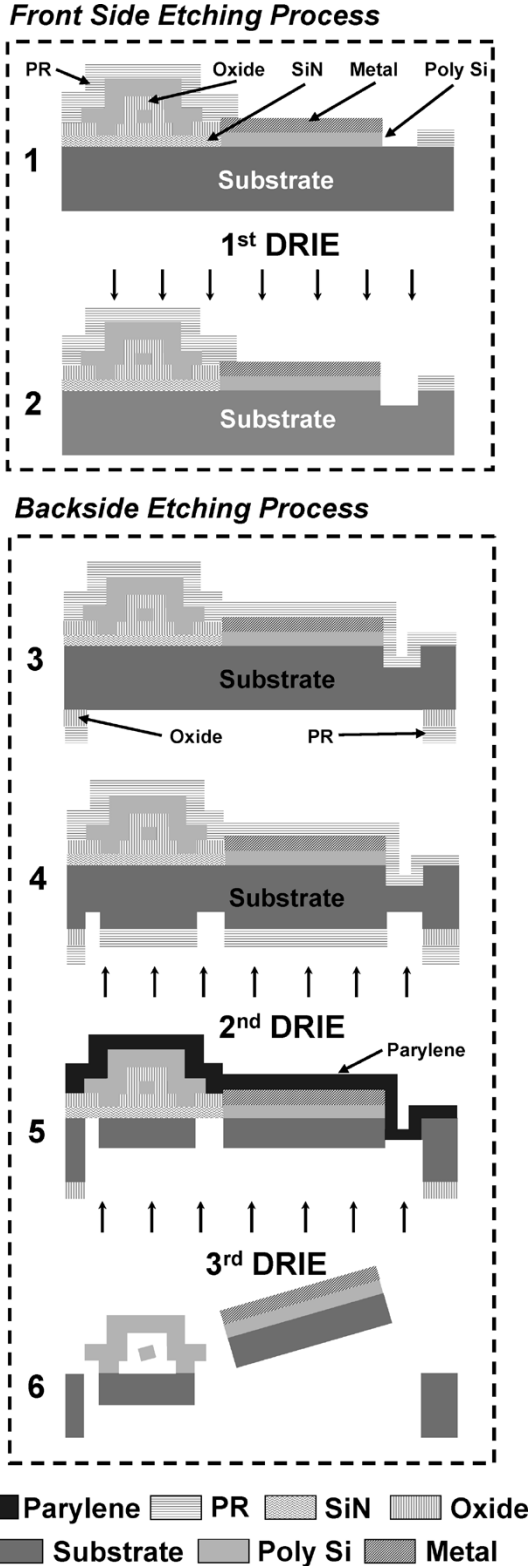


Fig. 7. Post fabrication process of the 2-D AVC scanner.

sured from their bottom edges. It is a function of the rotation angle, θ , and position, x

$$Z(\theta, x) = x \sin(\theta_i - \theta) - \left[L_{co} - \frac{T_f}{2} \tan(\theta) \right] \sin(\theta) + T_f(1 - \cos \theta_i). \quad (5)$$

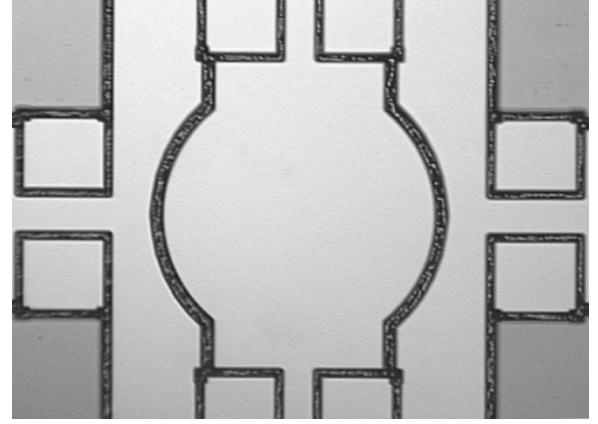


Fig. 8. Optical micrograph of the backside trenches after the second DRIE.

Therefore, C_t can be calculated by a finite integral as

$$C_t(\theta) = \int_{\frac{L_{fo}}{\cos(\theta_i - \theta)}}^{L_f} C_{\text{unit}}(Z(\theta, x)) dx \quad (6)$$

where L_{fo} , and L_{co} are the clearance and offset of the movable comb finger, respectively. We assume cross sectional areas are uniform over the entire rotation angle, and the lateral movement of the comb fingers are neglected.

C. Actuator-Flexure System

At equilibrium, the mechanical restoring torque is balanced by the electrostatic torque

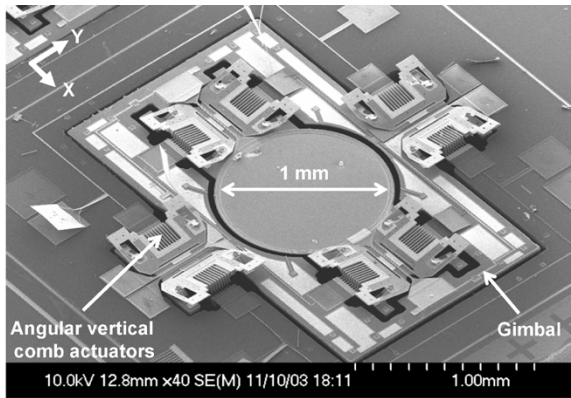
$$T_e(\theta, V) = T_r(\theta). \quad (7)$$

Therefore, the dc characteristic (θ versus V) of the scanner can be solved analytically. The calculated dc transfer curves for various torsion springs and comb finger lengths are shown in Fig. 5(a) and (b), respectively. The scanner parameters used in the calculations are listed in Table I.

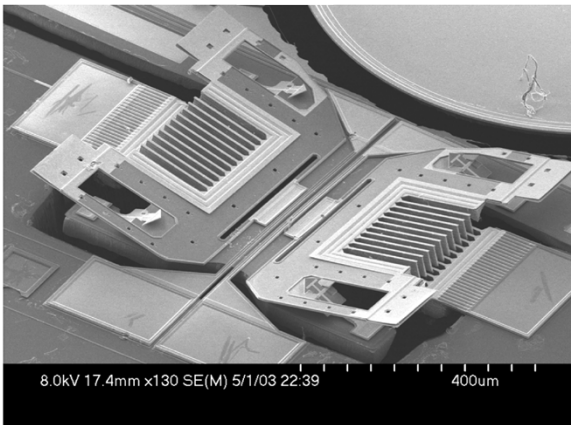
We employ polysilicon spring latches to precisely define the initial angle of the AVC. Bent polysilicon latches are fabricated using the *Poly2* layer in MUMPs. To avoid failure, the maximum stress of the bent beam is kept at 70% to 80% of the failure point (1.21 ± 0.8 GPa [23]).

IV. FABRICATION PROCESS

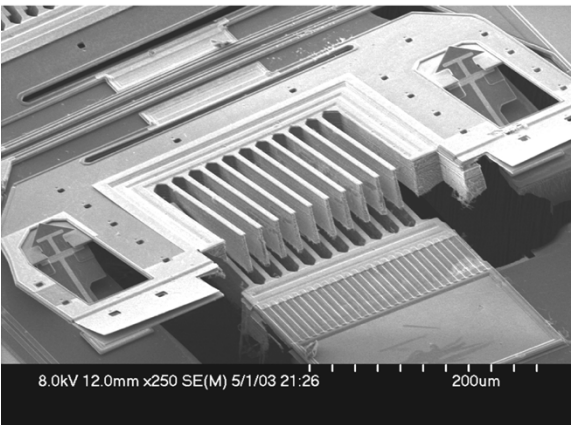
The surface-micromachining part of the fabrication process was realized by the MUMP's process. The bulk-micromachining processes are performed at University of California, Los Angeles (UCLA)'s Nanofabrication Facility. All lithographic steps in post-MUMP's processes are performed at die level. Multiple (4 to 6) dies are mounted on a handle wafer for dry etching process. The bulk-micromachining process is described in the following: first, the MUMP's chips ($550\text{-}\mu\text{m}$ -thick) thinned down to $300\ \mu\text{m}$ to reduce the backside etching time. This is performed in a Logitech PM5 chemical-mechanical planarization (CMP) System. Three polishing steps are employed to ensure a clean, smooth surface: first $9\text{-}\mu\text{m}$ Al_2O_3 is used for fast lapping, then $1\text{-}\mu\text{m}$ Al_2O_3 , and finally colloidal silica solution were used to polish and smooth the surface.



(a)



(b)



(c)

Fig. 9. SEM of (a) a 2-D AVC scanner, (b) outer comb and torsion beams, and (c) close-up view of a movable comb.

The final thickness of the polished MUMP's chips is $300\ \mu\text{m}$. The optical micrographs of the polished backsides are shown in Fig. 6. Final root-mean-square (rms) surface roughness of around $35\ \text{nm}$ is achieved, which helps prevent micromasking during subsequent backside etching.

The flow of the postfabrication process is shown in Fig. 7. First, the mirror, polysilicon hinges, torsion springs, and latches are protected by a $5\text{-}\mu\text{m}$ -thick photoresist (PR), SHIPLEY STR-1045, spun at 2250 RPM for 45 seconds, during the front-side etching (Mask 1). The metal patterns in MUMP's are used as the etching mask to define the comb fingers. The metal patterns

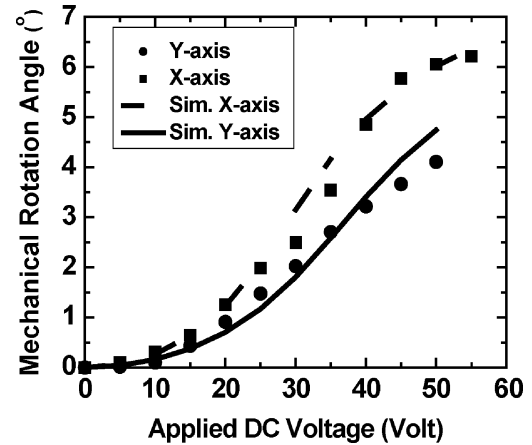


Fig. 10. Measured dc scanning characteristics of a 2-D AVC scanner.

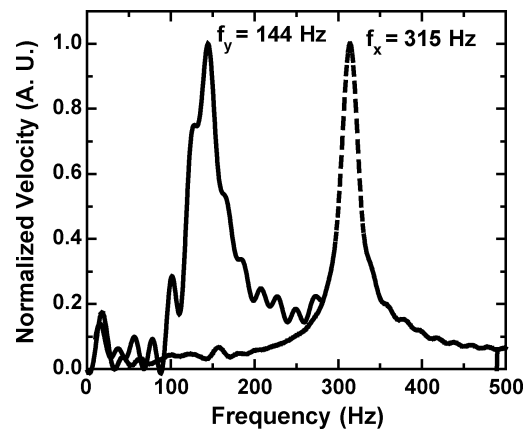


Fig. 11. Measured mechanical frequency response of a 2-D AVC scanner.

help ensure good alignments with the surface-micromachined structures. The comb fingers are timed (first DRIE) etched from the front side in a Unaxis SLR-770 ICP DRIE using the BOSCH process [28]. After the completion of the first DRIE, the PR is stripped in an acetone bath and then oxygen plasma is used to remove the PR remnants in a Matrix 105 Downstream Asher. The same PR is used for the rest of postfabrication process.

Next, a $2\text{-}\mu\text{m}$ -thick SiO_2 is deposited on the backside at 150°C in a Unaxis 790 plasma-enhanced chemical-vapor deposition (PECVD) system. Then, another PR is spun on the backside and patterned by the backside alignment feature on a Karl Suss MA-6 Aligner (Mask 2) to open the oxide areas underneath the mirror and the comb banks. The accuracy of the backside alignment is $\pm 5\ \mu\text{m}$ for the $1 \times 1\text{-cm}^2$ MUMP's chip (single die level lithography), which permits only a single objective lens of the Karl Suss Aligner due to a small die size. Anisotropic dry etching is performed on the backside of the die in an Oxford Plasmalab 80 Plasma Etcher to remove oxide openings until the polished SCS substrate is exposed. The backside of the die is exposed to a buffered oxide etchant (BOE) for 30 s to ensure complete removal of the PECVD oxide.

The PR is stripped off, and a new PR is spun on the backside. Mask 3 defines the SCS islands. A timed etch (second DRIE) is performed to delineate the SCS islands. To obtain a uniform etch, the gaps around the SCS islands are designed to have the same width ($30\ \mu\text{m}$). The trench depth is around $90\ \mu\text{m}$ after

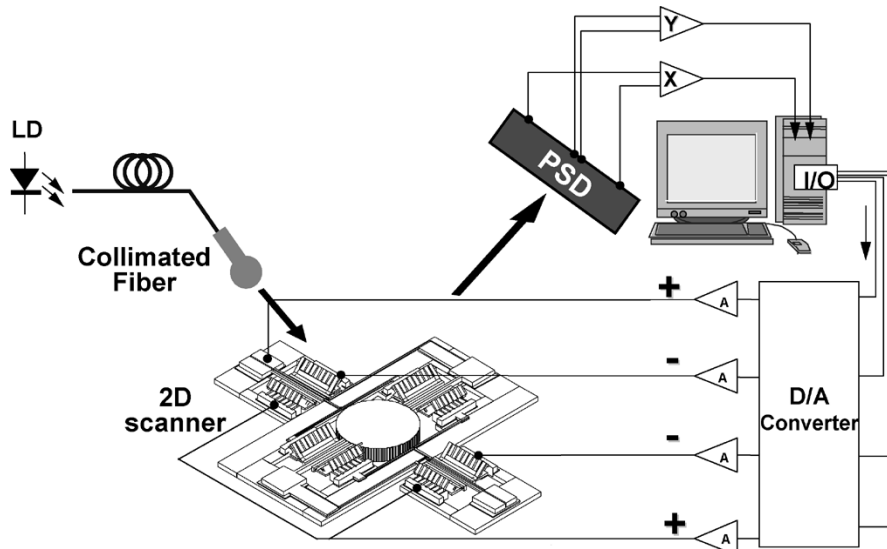


Fig. 12. Experimental setup for stability and repeatability measurements.

the completion of second DRIE. Fig. 8 shows the optical micrograph of the backside after the second DRIE. Then, the PR is removed from both sides, leaving the backside with previously patterned oxide. It is used as the hard mask in the final timed DRIE (third DRIE) step. The selectivity between the PECVD SiO_2 and the SCS is around 100 to 1 in DRIE.

A $1\text{-}\mu\text{m}$ -thick parylene is deposited on the front side in a Parylene Deposition System 2010 for mechanical support while the backside is protecting by a dicing blue tape. After the completion of Parylene deposition, the dicing blue tape is peeled off. The third DRIE step completely removes the substrate between the SCS islands (trenches). Due to the etching “lag” in the DRIE process, the large openings (unmasked SCS islands) will be etched faster than the small openings (pre-etch trenches from second DRIE). The etching rates for the unmasked SCS islands and preetch trenches are $3\ \mu\text{m}/\text{min}$ and $2.4\ \mu\text{m}/\text{min}$, respectively. An etching uniformity of 10% is achieved across the $1 \times 1\text{-cm}^2$ MUMPs’ chip. The remaining SCS islands are about $35\ \mu\text{m}$ thick.

Micromasking may be observed when the comb finger trenches produced by the front-side DRIE are exposed during the third DRIE. This comes from the residue passivation layer produced by the *BOSCH* process [28] during the front side etching. The micromasking creates silicon bridging sidewalls resulting in electrical short circuits between the fixed comb banks and the SCS substrate. To avoid this problem, oxygen plasma is used to etch away the passivation layers as soon as the front side etching trenches are exposed. Then, silicon isotropic etching processes, such as the *EtchB* step in the *BOSCH* process or the release step in the *SCREAM* process [29] is employed for a short period of time (1.5–2 min) to remove silicon micromasking.

The etching continues until it stops at the MUMP’s silicon nitride layer. The exposed silicon nitride is selectively removed by an anisotropic plasma etcher (Oxford Plasmalab 80 Plasma Etcher), which stops at the lower phosphosilicate glass (PSG1) layer in MUMP’s. Then, the scanners are diced into individual devices by a DISCO dicing machine. The device is released in 49% hydrofluoric (HF) acid for 15 min and dried in a supercritical dryer. The parylene layer is removed by oxygen plasma in

a Matrix 105 Downstream Asher. All movable comb banks are manually assembled to a pre-defined angle (10°) and locked in place by polysilicon latches. The scanning electron micrographs (SEMs) of the scanner, the close-up view of the AVC and the movable comb are shown in Fig. 9(a)–(c), respectively.

V. EXPERIMENTAL RESULTS

A. DC Characteristics

The dc characteristics (θ versus V) of the scanner were measured by a noncontact white light interferometric surface profiler (WYKO RST 500). Fig. 10 shows the measured (dots) and the calculated (lines) dc transfer curves for both axes. The measured results agree well with theoretical calculations. The initial comb angle of the assembled movable comb is designed to be 10° . The uniformity is measured to be within $\pm 0.7^\circ$. The maximum mechanical scanning ranges are $\pm 6.2^\circ$ (at 55 Vdc) and $\pm 4.1^\circ$ (at 50 Vdc) for the inner and the outer gimbals, respectively. The curvature radius of the 1-mm-diameter mirror is measured to be over 50 cm without metal coating. Larger radius of curvature and lower actuation voltage can be achieved by employing thicker mirror and comb fingers.

B. Dynamic Characteristics

The frequency responses were measured by a Polytech Microscan Laser Doppler Vibrometer (LDV) using the area-scan mode with periodically chirped voltage waveforms. The results are shown in Fig. 11. The resonant frequencies are measured to be 315 and 144 Hz for the inner and the outer gimbals, respectively, which match very well with the theoretical calculations.

C. Stability and Repeatability

One of the main issues of electrostatically actuated micromirrors is drifting of the mirror angle under a constant bias [30]. The drifting can be minimized by reducing the areas of the exposed dielectric [31], or using ac bias [3]. Our 2-D AVC scanner exhibits very small angular rotation drifts. The silicon nitride in comb fingers have been removed using standard MUMPs’ design rules to minimize dielectric charge-up.

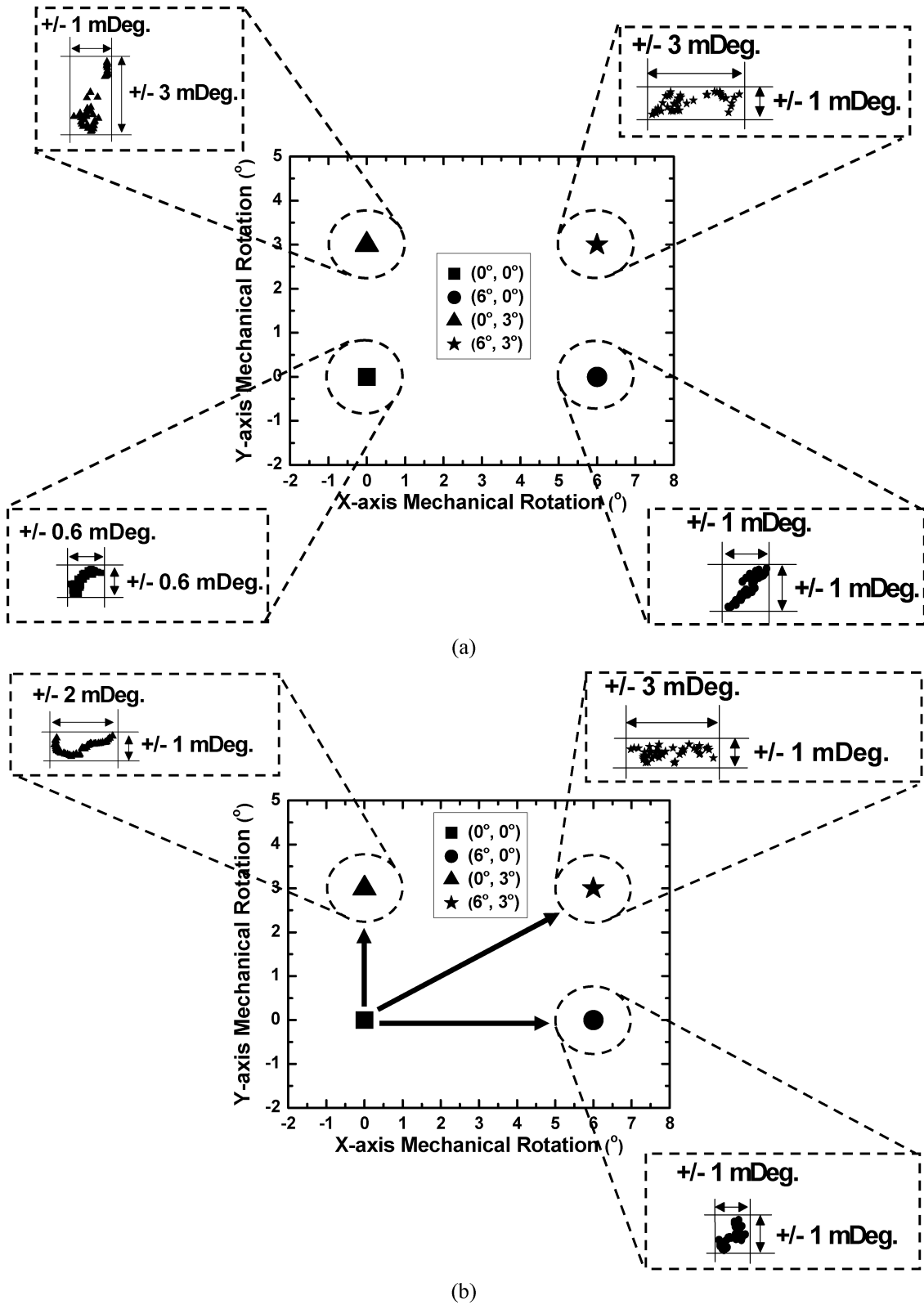


Fig. 13. Cumulative angular traces for (a) stability and (b) repeatability measurements for various bias angles.

The stability and repeatability of the scanner are characterized using a 2-D position sensing detector (PSD) (On-Trak 2L20SP). The experimental setup is shown in Fig. 12. The mirror is illuminated by a collimated red laser beam ($\lambda = 633 \text{ nm}$) from a laser diode. The reflected light is de-

tected by the PSD. The data acquisition was controlled by a personal computer using LabView from National Instruments.

The stability of the measurement setup is determined first using a bulk mirror. It is found to be less than $\pm 0.0001^\circ$. The stability of the scanner is measured by applying dc voltages, while

the repeatability is characterized by applying square waves with 50% duty cycles. For both measurements, the data is collected every 90 s for a total period of 1 h. The scanner stability is measured at four different scanner angles: (0°, 0°), (6°, 0°), (0°, 3°), and (6°, 3°). The variations of the mirror angles are shown in Fig. 13(a). The stability is better than $\pm 0.003^\circ$ for all angles, though the variation is found to be slightly larger at high voltage bias, e.g., at (6°, 3°). The repeatability of the mirror angle is measured when the mirror is switched between the origin, (0°, 0°), and three final angles: (6°, 0°), (0°, 3°), and (6°, 3°), as shown in Fig. 13(b). The repeatability of the mirror angles are found to be within $\pm 0.003^\circ$ for all angles. No systematic drifts are observed in the experiments.

VI. CONCLUSION

In this paper, we have successfully demonstrated a high-performance 2-D scanner with angular vertical comb (AVC) actuators by combining the surface- and the bulk-micromachining techniques. The scanner achieves fully decoupled x and y scanning with good stability ($< \pm 0.003^\circ$) and repeatability ($< \pm 0.003^\circ$). Large dc mechanical scan ranges ($\pm 6.2^\circ$ and $\pm 4.1^\circ$), low actuation voltages (55 and 50 Vdc), and large radius of curvature (> 50 cm) have been achieved for the 1-mm-diameter scanning mirror. The experimental results agree well the theoretical calculations.

ACKNOWLEDGMENT

The authors would like to thank J.-C. Tsai, S. Mathai, L. Fan, M. Fujino, and E. K. Lau of the University of California at Los Angeles (UCLA) for their technical assistance.

REFERENCES

- [1] Y. Mizuno, O. Tsuboi, N. Kouma, H. Soneda, H. Okuda, Y. Nakamura, S. Ueda, I. Sawaki, and F. Yamagishi, "A 2-axis comb-driven micromirror array for 3D MEMS switches," in *Proc. IEEE/LEOS Int. Conf. Optical MEMS*, Lugano, Switzerland, 2002, pp. 17–18.
- [2] D. M. Marom, D. T. Neilson, D. S. Greywall, N. R. Basavanahally, P. R. Kolodner, Y. L. Low, F. Pardo, C. A. Bolle, S. Chandrasekhar, L. Buhl, and C. R. Giles, "Wavelength-selective 1×4 switch for 128 WDM channels at 50 GHz spacing," in *Post Deadline Papers Optical Fiber Communication Conference*, Anaheim, CA, 2002, pp. FB7-1–FB7-3.
- [3] J. E. Ford, V. A. Aksyuk, D. J. Bishop, and J. A. Walker, "Wavelength add-drop switching using tilting micromirrors," *J. Lightw. Technol.*, vol. 17, no. 5, pp. 905–911, May 1999.
- [4] H. Toshiyoshi, K. Isamoto, A. Morosawa, M. Tei, and H. Fujita, "A 5-volt operated MEMS variable attenuator," in *Proc. Int. Conf. on Solid-State Sensors, Actuators and Microsystems*, Boston, MA, 2003, pp. 1768–1771.
- [5] M. H. Kiang, O. Solgaard, K. Y. Lau, and R. S. Muller, "Electrostatic combdrive-actuated micromirrors for laser-beam scanning and positioning," *J. Microelectromech. Syst.*, vol. 7, pp. 27–36, 1998.
- [6] L. J. Hornbeck, "Current status of the Digital Micromirror Device (DMD) for projection television applications," in *Proc. Int. Electron Devices Meeting*, 1993, pp. 381–384.
- [7] D. L. Dickensheets and G. S. Kino, "Silicon-micromachined scanning confocal optical microscope," *J. Microelectromech. Syst.*, vol. 7, no. 1, pp. 38–47, Mar. 1998.
- [8] W. Piyawattanametha, H. Toshiyoshi, J. LaCosse, and M. C. Wu, "Surface-micromachined confocal scanning optical microscope," in *Technical Digest Series of Conference on Lasers and Electro-Optics*, San Francisco, CA, 2000, pp. 447–448.
- [9] W. Piyawattanametha, P. R. Patterson, G. D. J. Su, H. Toshiyoshi, and M. C. Wu, "A MEMS noninterferometric differential confocal scanning optical microscope," in *Proc. Int. Conf. Solid-State Sensors, Actuators and Microsystems*, Munich, Germany, 2001, pp. 590–593.
- [10] W. Piyawattanametha, L. Fan, S. Hsu, M. Fujino, M. C. Wu, P. R. Herz, A. D. Aguirre, Y. Chen, and J. G. Fujimoto, "Two-dimensional endoscopic MEMS scanner for high resolution optical coherence tomography," in *Proc. Technical Digest Series of Conference on Lasers and Electro-Optics*, San Francisco, CA, USA, May 2004, CWS2.
- [11] L. Xingde, M. E. Brezinski, and J. G. Fujimoto, "High resolution optical imaging and spectroscopy of biological tissues," in *EMBS/BMES 2002, IEEE Engineering in Medicine and Biology Society/Biomedical Engineering Society Conference*, vol. 3, 2002, pp. 2241–2242.
- [12] H. Schenk, P. Durr, T. Haase, D. Kunze, U. Sobe, H. Lakner, and H. Kuck, "Large deflection micromechanical scanning mirrors for linear scans and pattern generation," *J. Sel. Top. Quantum Electron.*, vol. 6, no. 5, pp. 715–722, 2000.
- [13] S. Kwon, V. Milanovic, and L. P. Lee, "A high aspect ratio 2D gimbaled microscanner with large static rotation," in *Proc. IEEE/LEOS Int. Conf. Optical MEMS*, Lugano, Switzerland, Aug. 2002, pp. 149–150.
- [14] D. Lee and O. Solgaard, "Two-axis gimbaled microscanner in double SOI layers actuated by self-aligned vertical electrostatic combdrive," in *Proc. Technical Digest Solid-State Sensor, Actuator and Microsystems Workshop*, Hilton Head Island, SC, Jun. 2004, pp. 352–355.
- [15] V. Milanovic, G. A. Matus, T. Cheng, and B. Cagdaser, "Monolithic high aspect ratio two-axis optical scanners in SOI," in *Proc. Int. Conf. Micro Electro Mechanical Systems*, Kyoto, Japan, Jan. 2003, pp. 255–258.
- [16] D. Hah, P. R. Patterson, H. D. Nguyen, H. Toshiyoshi, and M. C. Wu, "Theory and experiments of angular vertical comb-drive actuators for scanning micromirrors," *J. Sel. Top. Quantum Electron.*, vol. 10, no. 3, pp. 505–513, May/June 2004.
- [17] P. Patterson, D. Hah, H. Nguyen, H. Toshiyoshi, R. Chao, and M. C. Wu, "A scanning micromirror with angular comb drive actuation," in *Proc. Int. Conf. Micro Electro Mechanical Systems*, Las Vegas, NV, Jan. 2002, pp. 544–547.
- [18] W. Piyawattanametha, P. R. Patterson, D. Hah, H. Toshiyoshi, and M. C. Wu, "A surface and bulk micromachined angular vertical combdrive for scanning micromirrors," in *Proc. Optical Fiber Communication Conference*, vol. 1, Atlanta, GA, Mar. 2003, pp. 251–252.
- [19] T. D. Kudrle, C. C. Wang, M. G. Bancu, J. C. Hsiao, A. Pareek, M. Waelti, G. A. Kirkos, T. Shone, C. D. Fung, and C. H. Mastrangelo, "Electrostatic micromirror arrays fabricated with bulk and surface micromachining techniques," in *Proc. Int. Conf. Int. Micro Electro Mechanical Systems*, Kyoto, Japan, Jan. 2003, pp. 267–270.
- [20] J. L. Yeh, H. Jiang, and N. C. Tien, "Integrated polysilicon and DRIE bulk silicon micromachining for an electrostatic torsional actuator," *J. Microelectromech. Syst.*, vol. 8, no. 4, pp. 456–465, 1999.
- [21] H. Xie, Y. Pan, and G. K. Fedder, "A SCS CMOS micromirror for optical coherence tomographic imaging," in *Proc. Int. Conf. Micro Electro Mechanical Syst.*, Las Vegas, NV, Jan. 2002, pp. 495–498.
- [22] G.-D. J. Su, H. Toshiyoshi, and M. C. Wu, "Surface-micromachined 2-D optical scanners with high-performance single-crystalline silicon micromirrors," *Photon. Technol. Lett.*, vol. 13, no. 6, pp. 606–608, 2001.
- [23] D. Koester, A. Cowen, R. Mahadevan, M. Stonefield, and B. Hardy, *PolyMUMP's Design Handbook*, 2003.
- [24] W. Piyawattanametha, P. R. Patterson, D. Hah, H. Toshiyoshi, and M. C. Wu, "A 2D scanner by surface and bulk micromachined angular vertical comb actuators," in *Proc. IEEE/LEOS Int. Conf. Optical MEMS*, HI, Aug. 2003, pp. 93–94.
- [25] K. S. J. Pister, M. W. Judy, S. R. Burgett, and R. S. Fearing, "Microfabricated hinges," *Sens. Actuators A, Phys.*, vol. 33, no. 3, pp. 249–256, 1992.
- [26] S. P. Timoshenko and J. N. Goodier, *Theory of Elasticity*, 3rd ed. New York: McGraw-Hill, 1970.
- [27] W. N. Sharpe Jr., "Measurements of Young's modulus, Poisson's ratio, and tensile strength of polysilicon," in *Proc. MEMS 97—Tenth IEEE International Workshop on Microelectromechanical Systems*, Nagoya, Japan, 1997, pp. 424–429.
- [28] R. B. Bosch GmbH, U.S. Pat. 4855017, U.S. Pat. 4784720, and Germany Pat. 4 241 045C1, 1994.
- [29] K. A. Shaw and N. C. MacDonald, "Integrating SCREAM micromachined devices with integrated circuits," in *Proc. Int. Conf. Micro Electro Mechanical Systems*, 1996, pp. 44–48.
- [30] J. Wibbeler, G. Pfeifer, and M. Hietschold, "Parasitic charging of dielectric surfaces in capacitive Microelectromechanical Systems (MEMS)," *Sens. Actuators A, Phys.*, vol. 71, pp. 74–80, 1998.
- [31] A. Gasparyan, H. Shea, S. Arney, V. Aksyuk, M. E. Simon, F. Pardo, H. B. Chan, J. Kim, J. Gates, J. S. Kraus, S. Goyal, D. Carr, and R. Kleiman, "Drift-free, 1000 G mechanical shock tolerant single-crystal silicon two-axis MEMS tilting mirrors in a 1000×1000 port optical crossconnect," in *Post Deadline Papers Optical Fiber Communication Conference*, Atlanta, GA, 2003, PD36-1 to PD36-3.



Wibool Piyawattanametha (M'03) received the M.S. and Ph.D. degrees in electrical engineering from the University of California, Los Angeles (UCLA), in 1999, and 2004, respectively. Prior to that, he received the B.Eng. (*magna cum laude*) in electronics engineering from King Mongkut's Institute of Technology Ladkrabang (KMITL), Bangkok, Thailand, in 1994.

From 1994 to 1997, he worked at Schlumberger, Ltd. He has authored or coauthored 20 conference and journal papers, and contributed a book chapter (coauthored with Dr. M. C. Wu) in the field of optical MEMS. He is currently with National Electronics and Computer Technology Center (NECTEC), 12120 Thailand, and Stanford University in the Bio-X program, CA 94305 USA as a research scientist. His research interests include Micro-Electromechanical Systems (MEMS), biomedical imaging systems, neuroscience, and photonics.



Pamela R. Patterson (M'04) received the B.S. degree (*cum laude*) from the University of Cincinnati, OH, and the M.S. and Ph.D. degrees in electrical engineering from the University of California, Los Angeles (UCLA), in 2003, completing the dissertation year as recipient of an Intel foundation fellowship.

She is currently a Research Staff Member at HRL Laboratories, Malibu, CA, conducting research on heterogeneous integration of semiconductor materials. Her research interests are in the area of microfabrication process design and technology and she has authored or coauthored 14 conference papers, including three invited papers, and contributed a book chapter (coauthored with Dr. M. Wu) in this field as applied to optical MEMS devices. She has held senior engineering positions at TRW, Varian, and at UCLA where she helped to establish the Nanoelectronics Research Laboratory from 1994 to 2003.

Dr. Patterson is a Member of AAAS and Eta Kappa Nu.



Dooyoung Hah received the M.S. and Ph.D. degrees in electrical engineering from the Korea Advanced Institute of Science and Technology (KAIST), Korea, in 1996 and 2000, respectively. His Ph.D. dissertation topic was a low-voltage RF MEMS switch.

He is currently an Assistant Professor of Electrical and Computer Engineering at Louisiana State University (LSU), Baton Rouge. Before joining LSU, he was with the University of California, Los Angeles, as a Postdoctoral Researcher (2000–2001) and as a Staff Research Associate (2004–2005), and at the Electronics and Telecommunications Research Institute (ETRI), Korea, as a Senior Member of the Research Staff (2002–2004). His research interests include MOEMS, RF MEMS, MEMS for biomedical applications, microactuators, sensors, and nanotechnology. He has authored and coauthored over 40 publications including journal papers and international conference proceedings, and he also holds five U.S. and six Korean patents.

Dr. Hah was the third-place winner at the Student Paper Competition at the 2000 IEEE MTT-S.



Hiroshi Toshiyoshi (M'97) received the M. Eng. and Ph.D. degrees in electrical engineering from the University of Tokyo, Tokyo, Japan, in 1993 and 1996, respectively.

In 1996, he became a Ph.D. Lecturer with Institute of Industrial Science (IIS), University of Tokyo. From April 1999 to March 2001, he stayed as a Visiting Assistant Professor at University of California, Los Angeles, for his sabbatical years. Since September 2001, he has been a Co-Director of IIS's Laboratory for Integrated MicroMechatronic Systems (LIMMS), a joint research group between IIS and Centre National de la Recherche Scientifique (CNRS), France. Since April 2002, he has been an Assistant Professor of VLSI Design and Education Center (VDEC) attached to University of Tokyo. His research interest is MEMS for free-space optics and nanomechanics.



Ming C. Wu (S'82–M'83–SM'00–F'02) received the B.S. degree in electrical engineering from National Taiwan University in 1983 and the M.S. and Ph.D. degrees in electrical engineering and computer sciences from the University of California, Berkeley, in 1985 and 1988, respectively.

From 1988 to 1992, he was a Member of Technical Staff at AT&T Bell Laboratories, Murray Hill. In 1993, he joined the faculty of Electrical Engineering Department of UCLA, where he is currently Professor. He is also Director of UCLA's Nanoelectronics Research Facility, and Vice Chair for Industrial Relations. His current research interests include MicroElectroMechanical Systems (MEMS), Optical MEMS (MOEMS), biophotonics, microwave photonics, and high speed optoelectronics. He has published over 340 papers, contributed four book chapters, and holds 11 U.S. patents.

Dr. Wu was the founding Co-Chair for IEEE LEOS Summer Topical Meeting on Optical MEMS in 1996. The meeting has now evolved into IEEE LEOS International Conference on Optical MEMS that are hosted in Europe, Asia, and U.S. He has also served in program committees of many other conferences, including Optical Fiber Communications (OFC), Conference On Lasers And Electrooptics (CLEO), IEEE Conference on Micro Electro Mechanical Systems (MEMS), LEOS Annual Meetings (LEOS), International Electron Device Meeting (IEDM), Device Research Conference (DRC), International Solid-State Circuit Conference (ISSCC), and Microwave Photonics (MWP) Conferences. He is a David and Lucile Packard Foundation Fellow (1992–1997).